Faraday Discussions

Cite this: *Faraday Discuss.*, 2025, **260**, 94

PAPER

Phytantriol and monoolein in aqueous deep eutectic solvent and protic ionic liquid solutions†

Karen J. Edler, ‡*[a] Gregory G. Warr, [b] Alexander M. Djerdjev, [b] Minh Thu Lam,[b] Adrian M. Hawley[c] and Stephen Mudie[c]

Received 10th January 2025, Accepted 22nd January 2025
DOI: 10.1039/d5fd00004a

Lyotropic liquid crystal gels of phytantriol and monoolein are well known examples of self-assembled systems in water, which have multiple applications across biomedical and materials science. However aqueous systems can be restricted by rapid solvent evaporation, and the limited solubility of some species in water. Here we explore the formation of liquid crystalline phases of phytantriol and monoolein in mixtures of water with two protic ionic liquids, ethylammonium nitrate (EAN) and ethanolammonium nitrate (EtAN), and three deep eutectic solvents (DES) formed from mixtures of choline chloride with urea, fructose or citric acid. The structures of the gel phase in excess solvent were measured using small angle X-ray scattering for a fixed lipid concentration (5% w/w) as a function of temperature. The phase diagrams of both lipids in DES–water mixtures and the non-amphiphilic ionic liquid, EtAN, indicate that higher negative curvature inverse hexagonal structures are favoured by addition of water. However, the amphiphilic ionic liquid EAN swells and stabilises the cubic *Pn3m* structure. The interplay of solvent structure, polarity and molecular size are key to understanding the formation and stability of lyotropic liquid crystalline gels in these systems.

Introduction

Phytantriol and monoolein are non-ionic amphiphiles which are well known for forming liquid inverse crystalline gel structures in the presence of excess water.[1,2] These species have complex phase behaviour which depends on their concentration, temperature, the presence of solutes such as salts and sugars, and other amphiphiles or hydrophobic species which can be incorporated into the lipid

[a]*Department of Chemistry, University of Bath, Claverton Down, Bath, BA2 7AY, UK. E-mail: karen.edler@chem.lu.se*
[b]*School of Chemistry, University of Sydney Nano Institute, The University of Sydney, NSW, 2006, Australia*
[c]*Australian Synchrotron, ANSTO, 800 Blackburn Road, Clayton, Victoria, 3169, Australia*

† Electronic supplementary information (ESI) available. See DOI: https://doi.org/10.1039/d5fd00004a

‡ Current address: Centre for Analysis and Synthesis, Department of Chemistry, Lund University, Sweden.

structure. The tunability of factors such as pore size and connectivity and the ability to maintain a three dimensional, connected liquid crystalline structure in a semi-solid gel state, in the presence of excess solvent, are key features which have driven application of these species in areas as diverse as templating of inorganic oxides[3] to drug delivery.[4] Both can be used to form colloidal particles of liquid crystalline phases known as cubosomes or hexosomes, depending on the structure within the particles. Such particles can be made, in the presence of a polymeric stabiliser, by breaking up bulk cubic or hexagonal phase gels, for instance *via* sonication, or by dripping solutions in a water miscible solvent, often ethanol, into water, where solvent exchange results in precipitation of particles with liquid crystalline structure. Phytantriol has higher cytotoxicity,[5] so is favoured for materials-focused applications such as electrodeposition of porous metal films,[6,7] antimicrobials[8] or cosmetic formulations.[9] Monoolein is better tolerated by cells and is seeing considerable investigation for delivery of poorly water-soluble drugs, vitamins and neutraceutical formulations and as peptide or protein supports. Monoolein also acts as a skin penetration enhancer and was recently used to promote transdermal delivery of powdered vaccines.[10]

The formation of gels using polar non-aqueous solvents is of growing interest in both the delivery of active species[11,12] and in materials applications, such as templating and electroplating. This has led us to explore and compare the structures formed by monoolein and phytantriol in excess solvent, using two classes of neoteric solvents, protic ionic liquids and deep eutectic solvents.

Protic ionic liquids (PILs) contain a cation with labile protons, such as ethylammonium, paired with either an aprotic or a protic anion, such as nitrate (NO_3^-), hydrogen sulfate (HSO_4^-) or amino acids. PILs are formed by proton transfer from a Brønsted acid to a Brønsted base, and thus are relatively straightforward to prepare, in addition to being chemically stable and having low toxicity.[13] Ethylammonium nitrate (EAN) is well known as the first ionic liquid in which micellization was studied.[14,15] In such PILs, coulombic interactions between opposite charges and hydrogen bonding combine to create a tunable solvophobic effect[16] that causes the expulsion of non-polar groups and drives the self-assembly of amphiphilic solutes.[17–20] In EAN and other alkylammonium ILs this induces amphiphilic nanostructure within the liquid itself, which is sensitive to cation and anion structure, and is largely eliminated by addition of the polar hydroxyl group to the cation to form ethanolammonium nitrate (EtAN).[21,22]

Deep eutectic solvents (DES) are liquids commonly formed from a mixture of a salt with a small neutral molecule. The mixtures have a lower melting point than either of the starting components, with strong intermolecular bonding resulting in a freezing point depression larger than that predicted by ideal mixing.[23] When two (or more) organic species are used, such as choline chloride and urea, the liquids are classed as Type III DES where hydrogen bonding interactions are key to the liquid properties.[24] DES are gaining interest as replacements for organic solvents due to their low volatility, relative chemical stability and the ability to form them easily using low cost, often bioderived, environmentally benign components. The ability to tune polarity by selection of the DES components and the fact that DES accommodate impurities such as water, solvated species and are often liquids for a range of ratios around the true eutectic composition, have led to investigation of these solvents for many applications. Initial work on DES focused on their use as solvents for electrodeposition of metals,[25] while other

studies have shown them to be useful for the synthesis of nanoparticles[26] and biomimetic inorganic materials.[27] Equally they can dissolve poorly water-soluble drugs,[28] stabilise proteins and enzymes in non-aqueous systems,[29] and have been suggested to contribute to the freeze and drought tolerance of plants and other organisms by providing a liquid with a lower freezing point than water, in which cell components can function.[30] The formation of self-organised lipid gels in these solvents may therefore have many applications in a wide range of areas, including materials synthesis and the development of novel therapeutic systems.

DES can also induce a solvophobic effect that supports amphiphilic self-assembly into micelles,[31] and lyotropic liquid crystalline phases by both cationic[32] and anionic surfactants.[33] Micelle size and shape are sensitive to the components of the DES,[34,35] but also depend on the surfactant counterion to a surprising extent, given the concentration of ions in the liquid.[36,37] Phospholipids have also been found to form stable vesicles in these solvents,[38,39] while biopolymers such as alginate[40] and cellulose nanofibrils[41,42] can be used to form eutectogels.

Until recently there has been little work on the formation of liquid crystalline phases of phytantriol and monoolein in DES. We have shown that 1 : 2 choline chloride : glycerol completely dissolves phytantriol, and this can be used for the anti-solvent regeneration of phytantriol cubosomes in water.[43] One other study reports cubic phases for phytantriol in choline chloride : urea, with an inverse hexagonal phase formed upon addition of water.[44] Work on the self-assembly of these two amphiphiles in PILs is more extensive.[45,46] Both monoolein and phytantriol were found to form 2D hexagonal phases in EtAN (phytantriol, 23–43 °C; monoolein 23–73 °C), while in EAN, bicontinuous cubic (35–60 °C) and lamellar (22–65 °C) phases were found for phytantriol but only a lamellar phase (<22–88 °C) for monoolein.[45] Cubosomes of both monoolein and phytantriol were also found in ethylammonium formate, forming a double diamond cubic and gyroid cubic mesophases.[47] Monoolein in ionic liquids prepared from choline or imidazole with aspartic acid or glutamic acid formed hexagonal, bicontinuous cubic and lamellar phases.[48] However, using alanine as the anion did not result in formation of any liquid crystalline phases, possibly due to degradation of the monoolein. Choline cations were more effective at inducing 2D hexagonal phases, with higher curvature interfaces than when imidazolium-based salts were used.[48] More recently, the formation of liquid crystalline structures in nanoparticles of monoolein prepared in mixtures of water and a range of PILs, then freeze dried, has been studied to determine how the cation and anion influence phase behaviour.[49] This study demonstrated that the presence of the PILs enabled the liquid crystalline nanoparticle structure to be retained upon freeze drying and compared behaviour of pure monoolein and monoolein/vitamin E acetate mixtures in water.

In this paper we examine the phase behaviour of phytantriol and monoolein gels in two PILs and three DES and their mixtures with water. We compare the archetypal choline chloride : urea (1 : 2), one of the most commonly studied DES, with choline chloride : fructose (1 : 1) and choline chloride : citric acid (1 : 1), as examples of sugar and organic acid-based DES, respectively. We have also probed the behaviour of these two lipids in the PILs ethylammonium nitrate and ethanolammonium nitrate, to explore how IL amphiphilic nanostructure affects liquid crystal stability. Structures formed by monoolein and phytantriol are

examined as a function of temperature and water content using small angle X-ray scattering to determine the role of each solvent component in the self-organisation of these systems.

Experimental

Phytantriol (purity >95%) was purchased from Adina Cosmetics Ingredients (Kent, UK), and monoolein (Cithrol, purity >96%) was a gift from Croda Chemicals (UK). Both were used as received, as were choline chloride (Sigma Aldrich, >98%), urea (AJAX, >99%), D-fructose (Univar analytical reagent), citric acid (Sigma Aldrich, 99%), ethylamine (Sigma, 70% in water) ethanolamine (Merck, >98%) and nitric acid (AJAX, AnalAR). Ultrapure water (18 MΩ cm) was used throughout.

Deep eutectic solvents choline chloride : urea (1 : 2; ChCl : U), choline chloride : fructose (1 : 1; ChCl : F) and choline chloride : citric acid (1 : 1; ChCl : CA) were prepared using standard methods. Briefly, the components were weighed into a clean, dry vial, which was sealed and mixed on a roller mixer at room temperature overnight before moving into an oven at 50 °C for 10 min (ChCl : U) or 2 h (ChCl : F, ChCl : CA) until clear homogeneous liquids were formed. The DES were then freeze-dried for 48 hours. Residual water contents (Karl Fischer titration) were 2.2% w/w in ChCl : U, 1.74% w/w in ChCl : CA and 1.15% w/w in ChCl : F.

Ethylammonium nitrate (EAN) and ethanolammonium nitrate (EtAN) were prepared as previously published,[14] *via* slow titration of the relevant amine base into aqueous nitric acid. The reaction was maintained below 10 °C in an ice bath. The pH of these aqueous solutions was maintained between 5 and 6, to prevent formation of amine-related impurities. Products were dried first to less than 5 wt % water content on a rotary evaporator, then under N_2 at 120 °C for 12 hours. Residual water in the EAN and EtAN was measured to be <0.3% w/w.

Each of the DES and PIL was diluted with water to form stock solutions ranging from 0 to 100% water (neglecting the initial water content) used to prepare mixtures containing 5% w/w phytantriol or monoolein, *i.e.* at a concentration of 0.05 g of amphiphile in 1 g total mixture after addition of solvent. Samples were equilibrated in the oven at 50 °C for 1 h and then at room temperature for 3 days before measurement. The sample state was noted to be unchanged after a further 6 weeks at room temperature. Observed behaviour varied from swelling of the amphiphile, which remained as a distinct gel phase (or phases) coexisting with excess solvent or solution, to complete dissolution.

Small angle X-ray scattering patterns were taken on the SAXS/WAXS beamline at the Australian Synchrotron using 12 keV X-rays (~1 Å wavelength), and 1 second exposures, recorded on a Dectris-Pilatus 1 M detector. Data was reduced from the 2D image to 1D patterns using the ScatterBrain software,[50] calibrated using measurements of silver behenate. Samples were held in perforated 2 mm thick aluminium plates with sticky Kapton sheets forming windows, and were measured at 25, 30, 40 and 50 °C, starting from the lowest temperature and commencing measurements only after 20 min equilibration at each temperature. Where the solution contained two phases, the gel phase was sampled for the SAXS measurements rather than the supernatant solution. Where required, a background consisting of an empty cell with Kapton windows was subtracted from the data.

Results

The three DES and two PILs were selected to cover a range of liquid types with different polarities and interactions with phytantriol and monoolein. The chemical structures of all components used are shown in Fig. 1. Choline chloride-based DES are the most commonly studied DES due to their low cost and generally low toxicity. ChCl : U (1 : 2, m.p. 23.5 °C)[51,52] and ChCl : F (1 : 1, m.p. 327.62 K, 54.47 °C)[53] are at their eutectic compositions in this study, while ChCl : CA at 1 : 1 molar ratio is liquid; after our study was performed, the eutectic composition for this solvent was determined to be 2 : 1 ChCl : CA.[54] The published phase diagram indicates that the melting point at 1 : 1 is 364.05 K (90.9 °C), while the eutectic ratio melts at 343.55 K (54.47 °C).[54] All of these pure liquids, when dry, are thus supercooled at room temperature, but no crystallisation was observed even during storage for several weeks after the beamtime measurements. Once water is added, the melting points decrease and at the water concentrations used here, all of the melting points are well below room temperature.[51,53,55]

Our earlier work has demonstrated that self-assembly of ionic surfactants can occur in ChCl : U as well as in choline-based DES with glycerol or organic acids while protic ionic liquids such as EAN and EtAN have also been demonstrated to support micellization. However, we note that in the choline chloride-based DES, non-ionic ethylene oxide based amphiphiles generally have extremely low solubilities, so the solubility of the non-ionic phytantriol and monoolein is unexpected.

The identities of the self-assembled phases and lattice parameters formed by monoolein and phytantriol in the five mixed solvent systems, determined by indexing the peaks of lyotropic phases, are shown in Fig. 2–9. Micellar solutions were identified by the characteristic shoulder and broad peak scattering that was

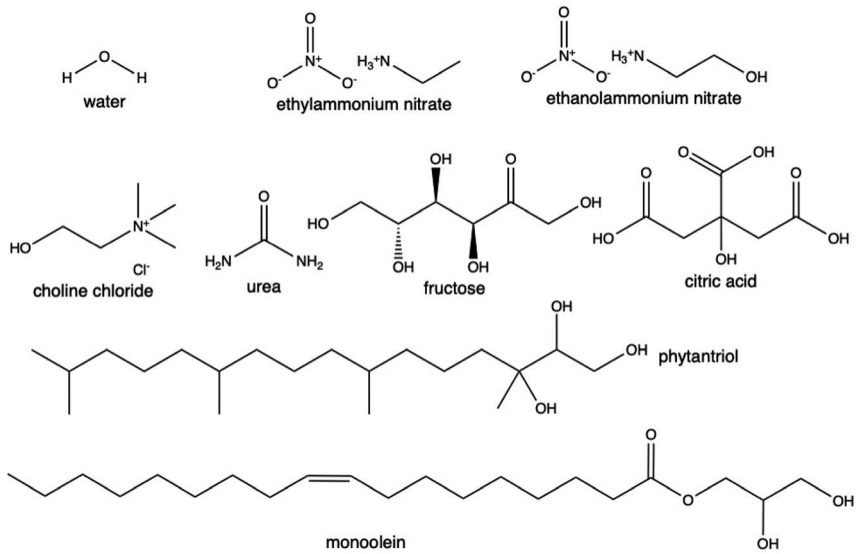

Fig. 1 Structures of the various components studied in this work.

well described by a fit to a spherical core–shell model of electron densities, indicating a hydrocarbon tail filled core *i.e.* normal rather than inverse micelles. We have not reported fit parameters, as neutron scattering with isotopic labelling would be required to reliably determine these. All diffraction patterns are shown in ESI Fig. S1–S10.†

Ionic liquids: ethylammonium nitrate (EAN) and ethanolammonium nitrate (EtAN)

Monoolein. Fig. 2 shows the phases observed in 5% w/w monoolein in (a) EtAN/water and (b) EAN/water solvent mixtures. Monoolein in water shows only the expected *Pn*3*m* (Q^{224}) cubic phase[56] at all temperatures examined. In pure EtAN an inverse hexagonal (H_{II}) phase is instead formed, which is consistent with a polarising optical microscopy study by Greaves *et al.*[45] on Myverol (a mixture containing ~70% monoolein).

As EtAN content increases, the *Pn*3*m* cubic phase is retained down to ~40% w/w water content at 25 °C (Fig. 2), with the H_{II} phase forming below ~20% w/w water. At 30% w/w cubic and hexagonal phases are found in three-phase coexistence with excess solvent. Upon warming, the cubic phase recedes towards the water axis as the H_{II} phase expands and the three-phase coexistence region shifts accordingly. Partial ternary phase diagrams for all systems are shown in ESI (Fig. S11–S14†) and were constructed combining the present data with available literature.

Fig. 3 shows that the lattice parameter for the *Pn*3*m* cubic phase decreases only slightly with increasing EtAN content, and this effect diminishes on warming, indicating only a small decrease in the maximum swelling of this phase. The decrease in lattice parameter is, however, more pronounced in the H_{II} phase, which forms at higher EtAN content (Fig. 3). This indicates that more highly curved aggregates form in EtAN than in water, supporting the suggestion that EtAN favours the H_{II} phase while water leads to the *Pn*3*m* cubic structure.

While addition of EAN to monoolein also preserves the *Pn*3*m* cubic phase down to 50% w/w, beyond this it behaves very differently to EtAN. In pure EAN and 10% water, a power law decay with a slope of −2 is observed. This is consistent

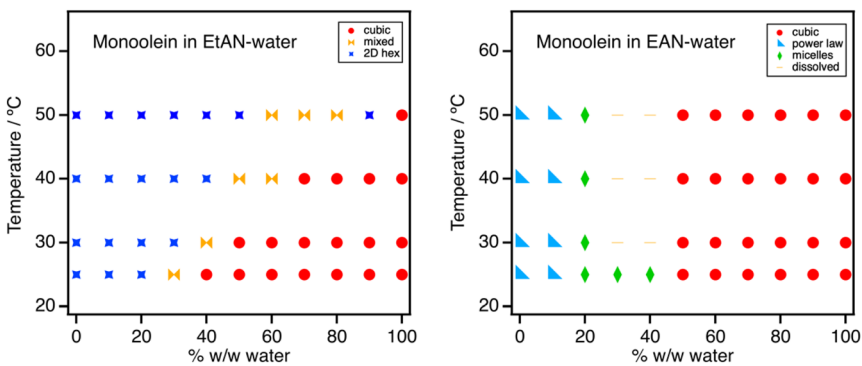

Fig. 2 Phases formed by 5% w/w monoolein in (left) EtAN– and (right) EAN–water mixtures. Schematic isothermal ternary phase diagrams drawn combining our data with available literature are shown in Fig. S11.†

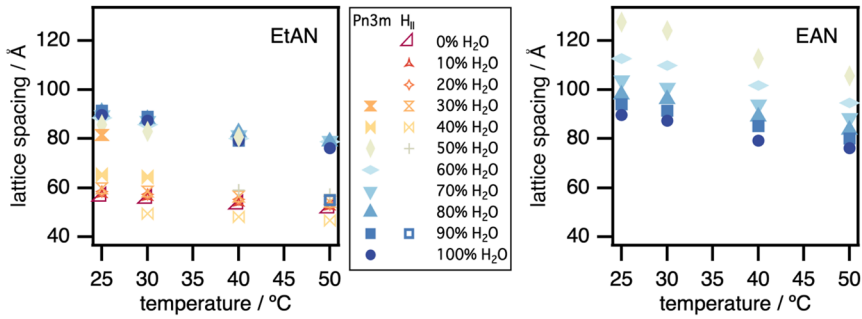

Fig. 3 Lattice spacings for the swollen *Pn3m* cubic and H_{II} phases for monoolein in excess EtAN–water and EAN–water mixtures. The error bars are smaller than the marker sizes.

with sheet-like structures which may indicate vesicles,[57] that could result from a dilute dispersion of monoolein lamellar phase, as reported by Greaves *et al.*, from polarising optical microscopy of Myverol in pure EAN.[45] We note that one of their images does show myelinic figures often seen prior to vesicle budding,[45] and also that Myverol contains only 70% monoolein, and may contain components that affect phase behaviour, as has been shown for phytantriol.[58] At intermediate EAN content of 20–40% w/w water, a broad peak is seen, indicating a homogeneous micellar solution. This is consistent with previous reports of micelle formation in EAN by hydrophobic amphiphiles such as phospholipids[59,60] and catanionic surfactants.[61] The phases formed in EAN/water mixtures are almost insensitive to temperature in the range studied.

In contrast to EtAN, the *Pn3m* phase lattice parameter increases markedly with EAN addition, from ~90 to ~125 Å. This means that the phase is more swollen by solvent and so much less curved at high EAN content. The size of the polar solvent domains within such cubic phases can be calculated using the method of Turner *et al.*[62] Assuming that the alkyl chain length of 17 Å of monoolein[63] depends little on solvent composition, the solvent channel diameter increases from 36 Å in water to 63 Å in 50/50 EAN/water.

Ethylammonium is known to act as a cosurfactant that favours more positively curved interfaces, *e.g.*, stabilising micelles over planar bilayers;[59–61] its uptake could thus also reduce the negative curvature of the bilayer within the *Pn3m*, enabling more solvent swelling before inducing the transition to a lamellar phase. EAN–water mixtures are also known to retain EAN's inherent amphiphilic nanostructure up to high water dilutions.[64,65] Larger polar solvent domains within the *Pn3m* phase would favour accommodating such a nanostructured solvent, with its own periodicity of ~10 Å,[64,65] and could enhance the stability of the more swollen structure.

The lattice parameter of the monoolein *Pn3m* phases in EAN–water mixtures decreases slightly with increased temperature (Fig. 3). This corresponds to the decrease in its maximum swelling in water, and is much smaller than the effect of changing solvent composition.[56,63]

Phytantriol. Fig. 4 shows the phases observed in 5% w/w solutions of phytantriol, a shorter chain lipid, which is liquid at room temperature, in EtAN and EAN water mixtures. Phytantriol in pure water exhibited a *Pn3m* (Q^{224}) cubic phase

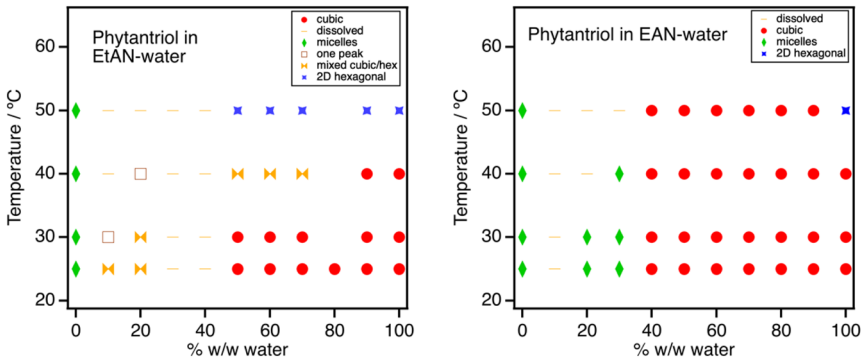

Fig. 4 Phases formed by 5% w/w phytantriol in EtAN–water (left) and EAN–water (right) mixtures. Schematic isothermal ternary phase diagrams are shown in Fig. S12.†

from 25–40 °C which became the inverse hexagonal phase, H_{II} at 50 °C, consistent with previous studies.[2] Phytantriol forms micellar phases in neat EAN and EtAN.

As water is added to EtAN, small amounts of coexisting ordered phases are observed. Where there are sufficient peaks for these to be assigned, we identify coexisting inverse hexagonal H_{II} and cubic *Pn3m* lyotropic phases at lower water content, then *Pn3m* only. This is consistent with Greaves *et al.*[45] identification of a H_{II} phase for phytantriol in pure EtAN; indeed a single small peak at $Q = 0.138$ Å^{-1} can be discerned upon close inspection of the scattering from pure EtAN, close to that of the adjacent cubic phase in the 10% w/w water, sample suggesting that this could result from a trace amount of the *Pn3m* phase coexisting with the micellar solution. As temperature increases, the H_{II} phase is detected in more water-rich samples and the *Pn3m* phase recedes towards the water axis. At 50 °C, the *Pn3m* phase is no longer present as H_{II} becomes the stable phase in water above 43 °C,[2] but has melted in EtAN.[45]

Fig. 5 shows that *Pn3m* lattice parameters for phytantriol in EtAN/water mixtures are close to those in pure water at 25 °C (between *ca.* 60–70 Å), as with monoolein, and decrease slightly as the temperature is increased, although more slowly than in water. It has been previously observed that addition of inorganic

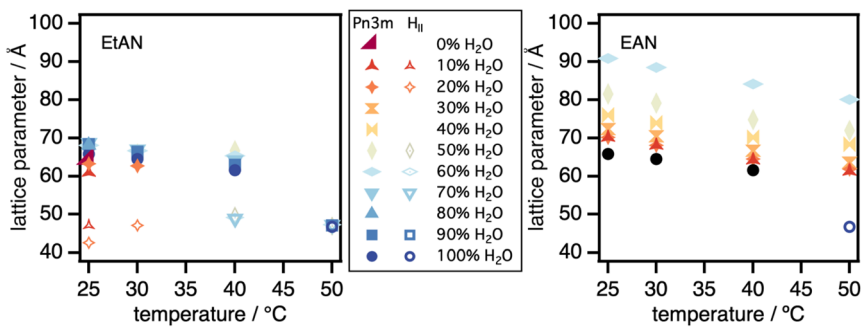

Fig. 5 Lattice parameters of the *Pn3m* cubic and H_{II} phases observed for phytantriol in EtAN–water and EAN–water mixtures. The error bars are smaller than the marker sizes.

salts such as hexachloroplatinic acid (in 8% w/w aqueous solution) at room temperature do not alter the observed lattice spacing for the *Pn3m* phase in phytantriol,[7] which is consistent with EtAN acting as a simple salt in this mixture.

In EAN, micelles are observed up to 30% w/w water. At higher water content, a *Pn3m* cubic phase is again observed in equilibrium with excess solvent. Greaves *et al.*[45] have reported both cubic and lamellar phases for phytantriol in pure EAN in flooding experiments. These must occur at higher phytantriol concentrations than used here, where we see only a micellar solution. This, as well as the stability of the micellar phase towards added water, is consistent with EAN's well-established ability to stabilise micelles of phospholipids.[59,60]

Fig. 5 shows that, as with monoolein but in contrast to EtAN, the *Pn3m* lattice parameters of phytantriol increase markedly with EAN addition (from *ca.* 65–90 Å). Using a length of 14 Å for the shorter phytanyl chain, this corresponds to an increase in polar domain diameter from 23 Å in water to 43 Å at 60% w/w EAN. As noted above for monoolein, the amphiphilicity of EAN enables it to stabilise more swollen, lower curvature structures, which may continue to yield even larger spacings at higher phytantriol contents, coexisting with the micellar solution phase. As with monoolein, there is again a monotonic decrease in lattice spacing with increasing temperature; spacings at 50 °C are 8–10 Å smaller than at 25 °C. Interestingly, EAN also stabilises the lower-curvature *Pn3m* cubic phase of phytantriol at 50 °C which has already transitioned to a H_{II} phase in pure water.

Deep eutectic solvents: choline chloride + urea/fructose/citric acid

So far there is little work reported on phytantriol or monoolein self-assembly in DES. Bryant *et al.*[44] explored the phase diagram for phytantriol in ChCl : U with varied amounts of water, and similarly found the formation of liquid crystalline phases, discussed in comparison to our results below. We are not aware of other studies so far on these lipids in other DES.

In general, the phase diagrams of both lipids in DES–water mixtures follow similar patterns to that seen with the non-amphiphilic ionic liquid, EtAN; higher negative curvature is favoured by moving from water into DES. We consider each lipid in turn below, in the three deep eutectic solvents choline chloride : urea, choline chloride : fructose and choline chloride : citric acid.

Monoolein. For monoolein, at low temperatures, a diversity of behaviour is seen among the three different DES (Fig. 6). As ChCl : U content increases, the swollen *Pn3m* phase, stable in water at all temperatures studied here, gives way first to three-phase coexistence of *Pn3m* with the H_{II} phase, and then to the H_{II} phase alone in excess solvent, above 40 °C. This behaviour is similar to that of monoolein in EtAN (Fig. 2). Ternary isothermal phase diagrams (Fig. S13†) show that, like monoolein in EtAN, as the *Pn3m* phase shrinks towards the water axis and the H_{II} phase expands from the ChCl : U axis upon warming, the solvent in the three-phase coexistence region also becomes more water-rich. Strikingly, coexisting *Pn3m* and H_{II} phases are seen even in 100% ChCl : U at 25 and 30 °C. This means that the transition temperature of the (low T and more swollen) *Pn3m* to (high T and less swollen) H_{II} in pure DES must lie in this temperature range, so that both phases are slightly out of equilibrium as they exchange solvent (see Fig. S15†). Coexisting phases detected at 10% w/w water and at higher temperatures also suggest that some systems have not fully equilibrated.

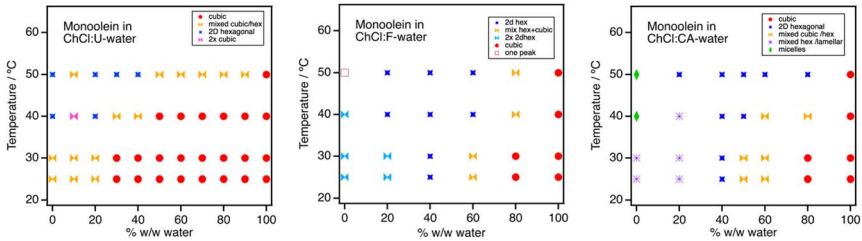

Fig. 6 Phases observed in 5% w/w monoolein in ChCl : U–water, ChCl : F–water and ChCl : CA–water mixtures. Schematic isothermal ternary phase diagrams are shown in Fig. S13.†

Fig. 7 shows that the ChCl : U cubic phase has lattice spacings that are very similar to those in the aqueous systems at all temperatures. This means that, like in EtAN, the maximum swelling of the phase is not sensitive to solvent composition. The H_{II} lattice spacing of 60 Å in most samples is also similar to that in water/EtAN mixtures, and also in water alone, where this phase forms at higher temperatures. Briggs *et al.* report 52.8 Å for a monoolein H_{II} phase at 97 °C for 78% w/w lipid,[63] while Larsson *et al.*[66] reports maximum swellings for monoolein

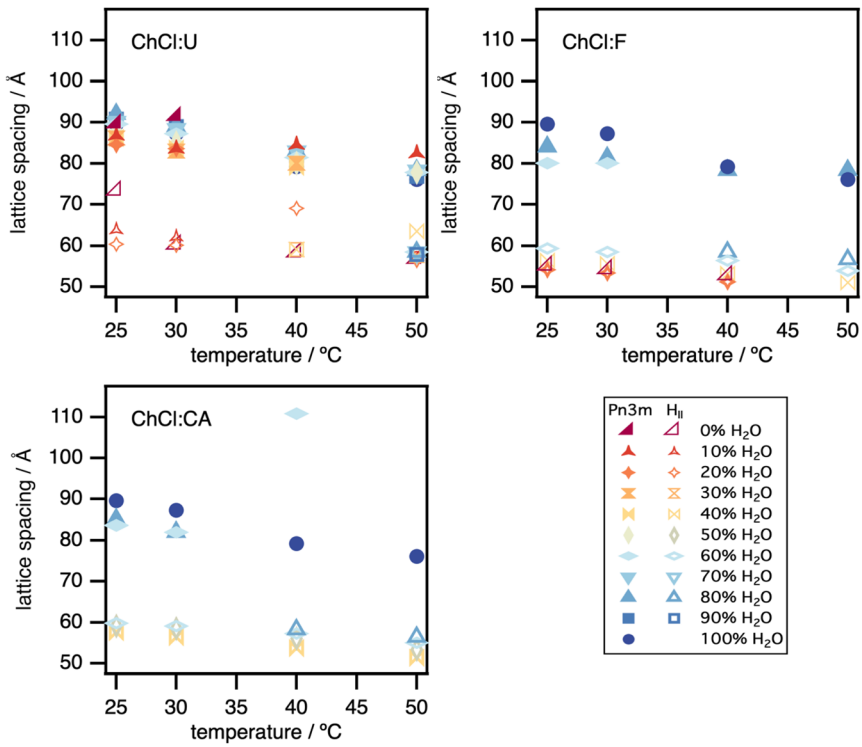

Fig. 7 Lattice spacings for the *Pn3m* cubic and H_{II} phases observed for monoolein in ChCl : U–water, ChCl : F–water and ChCl : CA–water mixtures. The error bars are smaller than the marker sizes. Where two H_{II} phases are observed, the larger lattice spacing is plotted.

(sunflower oil monoglyceride) of 58.2 Å at 45 °C and 47.9 Å for H_{II} at 75 °C for 60% w/w lipid. However, spacings found in some of our samples in or near three-phase coexistence, including 100% ChCl : U at 25 °C, are much larger. This also suggests that the H_{II} phase in pure ChCl : U becomes stable and more swollen at lower temperatures. In water, where H_{II} occurs at much higher temperature, lattice spacing also decreases upon warming; this may explain why the spacing in ChCl : U at lower temperatures is so much larger.

The phase behaviour of monoolein in ChCl : F is similar to that in ChCl : U, although the swollen *Pn3m* cubic phase is relatively less and the H_{II} phase more stable. *Pn3m* thus gives way to three-phase coexistence with H_{II} and to H_{II} only at lower water contents. In 100% ChCl : F and ChCl : F-rich samples at lower temperatures, diffraction patterns can be indexed to two hexagonal phases with slightly different spacings or swellings. This may be due to slow equilibration in such a high viscosity liquid.

The lattice spacings (Fig. 7) of the cubic phase decrease markedly from their value in pure water near room temperature with ChCl : F addition, meaning that the phases are less swollen. As these spacings also decrease in water with increasing temperature, the differences become less. In the ChCl : F-rich H_{II} phase, spacings increase slightly as water content increases. Saturni *et al.*[67] have shown that the lattice parameters of monoolein *Pn3m* phases also shrink in the presence of various sugars and suppress the transition to *Ia3d*. They attribute this to sugars altering the interfacial geometry of the lipid film.

ChCl : CA has the most complex phase behaviour of the solvents examined. Like ChCl : F, addition of ChCl : CA rapidly destabilises the *Pn3m* phase in water in favour of H_{II}, but in ChCl : CA-rich mixtures we detect micelles at high temperatures and lamellar structures at lower temperatures. In 100% ChCl : CA we find a lamellar order with a repeat spacing of 44 Å, which agrees with the 43.6 Å reported by Briggs *et al.*[63] for the low-temperature L_c phase of monoolein. At low water content we also find lamellar phases (likely L_α) coexisting with the H_{II} phase and excess mixed solvent. The phase and coexistence regions are shown with ternary diagrams in Fig. S13.† Lattice spacings decrease with addition of ChCl : CA in both *Pn3m* and H_{II} phases, but less markedly than ChCl : F in both cases. Here also, these only slightly decrease with increasing temperature.

Phytantriol. Fig. 8 shows that, like monoolein, the phase behaviour of phytantriol in mixed DES/water solvents also shows a sensitivity to choice of molecular component.

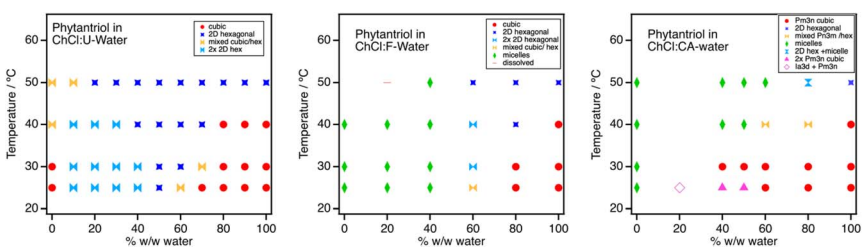

Fig. 8 Phases observed for 5% w/w phytantriol in ChCl : U–water, ChCl : F–water and ChCl : CA–water mixtures. Schematic isothermal ternary phase diagrams are shown in Fig. S14.†

The behaviour of 5% w/w phytantriol in ChCl : U/water mixed solvent is mostly similar to that reported by Bryant *et al.*[44] for 10% w/w solutions. In pure water, our data shows that the *Pn3m* cubic phase melts entirely below 50 °C and forms an H_{II}, in agreement with earlier work by Barauskas and Landh,[2] whereas Bryant *et al.* reported the *Pn3m* cubic phase remaining stable up to at least 70 °C in water.[44] In pure ChCl : U we also find a *Pn3m* cubic phase as reported by Bryant *et al.*, although at 50 °C, our sample formed coexisting cubic and H_{II} phases. This coexistence remains in 10% w/w water but has transformed completely to H_{II} by 20% w/w.

The H_{II} phase dominates the phase behaviour at intermediate solvent compositions. It is not present at lower temperatures in water, and if stable in pure ChCl : U it must lie at higher concentration than *Pn3m*. The water-rich *Pn3m* phase can be swollen by ~30% w/w DES, but the ChCl : U *Pn3m* phase can tolerate <10% w/w water before forming H_{II}. SAXS patterns of ChCl : U-rich samples at lower temperatures showed two co-existing H_{II} phases, with a small offset in lattice spacing. It seems unlikely that these systems can be truly equilibrated, since such structures would require segregation of different solvent components to give structures with different lattice spacings. These may represent H_{II} phases formed in different regions of the sample due to incomplete mixing at the time of measurement, *e.g.* one set of peaks is H_{II} in equilibrium with excess solvent while the other is adjacent to liquid phytantriol. A second explanation could be that adding water to the cubic phase of 100% ChCl : U forms coexisting DES-rich and water-rich H_{II} phases. This would imply a H_{II} phase in the binary ChCl : U–phytantriol phase diagram at slightly higher concentration (with smaller lattice spacing than the cubic), in addition to the water swollen H_{II} phase seen at high water contents.

Interestingly, ChCl : U is the least viscous of the DES studied here (see Table S1,† ESI for DES properties), so should have less diffusion limitation for reaching the equilibrated state. However, as described below, both ChCl : F and ChCl : CA support micelle formation in addition to the liquid crystalline phases. Higher solubility of phytantriol in these solvents should thus speed equilibration compared to ChCl : U, despite their higher viscosity.

Lattice spacings for phytantriol in ChCl : U (Fig. 9 below) also largely agree with those reported by Bryant *et al.*[44] The lattice parameter in the fully swollen *Pn3m* phase is ~65 Å and the H_{II} phase is ~45 Å in all mixtures, independent of composition. The striking result arises in pure ChCl : U, where the lattice parameter for both the *Pn3m* phase (~75 Å), and the H_{II} phase, seen at high temperatures, (*ca.* 51 Å) are much larger than in samples containing any amount of water. In the *Pn3m* phase this corresponds to an increase in polar domain diameter from 23 Å in water-rich structures to 30 Å in pure ChCl : U.

In ChCl : F and ChCl : CA, the trends broadly follow those seen for phytantriol in ChCl : U, but with less water required to transform *Pn3m* into H_{II} at any temperature. Phytantriol also forms micelles in both ChCl : F and ChCl : CA-rich solvent mixtures. This mirrors its behaviour in EAN–water mixtures and in pure EtAN.

In ChCl : F, micellar phases are observed below 60% w/w water. Beyond this, coexisting *Pn3m* cubic and H_{II} phases at 25 °C yield two hexagonal phases at 30 and 40 °C, before forming a single H_{II} phase at 50 °C. As noted above, the coexisting hexagonal phases were likely not completely equilibrated on the

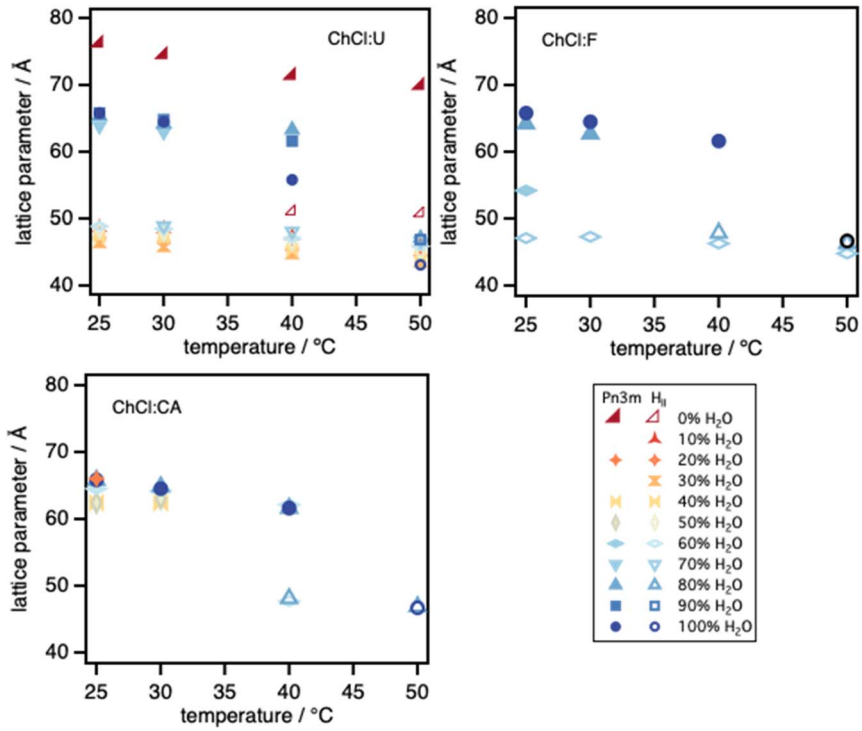

Fig. 9 Lattice spacings for the *Pn*3*m* cubic and H_{II} phases observed for phytantriol in ChCl : U–water, ChCl : F–water and ChCl : CA–water mixtures. The error bars are smaller than the marker sizes.

timescale of the experiment. Further water addition yields the cubic phase at low temperatures, and the DES lowers the transition temperature from the cubic phase to H_{II}.

In ChCl : CA, micellar solutions extend up to 50% w/w water at 40 and 50 °C. Unfortunately, the sample at 20% w/w water was not measured during the synchrotron experiment, but a measurement at 25 °C on a lab-based instrument taken after several weeks equilibration time, showed the coexistence of *Pn*3*m* and *Ia*3*d* phases, also seen by others for phytantriol in water.[2] Further increase in water content yielded a *Pn*3*m* phase, but at 25 °C doubling of the peaks suggests this phase was also not fully equilibrated. Heating to 30 °C allowed equilibration to the *Pn*3*m* cubic phase for all water contents higher than 40% w/w although again, the presence of the DES promotes melting of this phase either directly into micelles, or, at 60% w/w water or above, into H_{II} phases.

Lattice spacings of lyotropic phases of phytantriol in ChCl : F and ChCl : CA mixed solvents are in most cases very close to those in water. The *Pn*3*m* cubic lattice spacings lie between *ca.* 62–66 Å and H_{II} between *ca.* 44–48 Å (Fig. 9), decreasing slightly with increasing temperature. The lattice spacing for the *Ia*3*d* phase seen for phytantriol in 20% w/w water in ChCl : CA at 25 °C is 100.6 Å, similar to that reported by Barauskas and Landh,[2] who found an *Ia*3*d* phase with a lattice spacing close to 100 Å, at a water concentration of 23% w/w at 22 °C.

Discussion

Changing solvent and mixed solvent composition gives rise to a diverse range of phase behaviours in the gel phase of these lipids. Among the solvents examined, only EAN, EtAN and ChCl : U could be incorporated to any significant degree into the lyotropic cubic phases of either phytantriol or monoolein. Addition of EtAN or ChCl : U to aqueous systems yielded similar phase equilibria and temperature dependence, with only small changes in lattice parameters.

This contrasts markedly with EAN, which increases the *Pn*3*m* lattice parameter, corresponding to a less curved lipid film and an increase in the diameter of solvent domains of 27 Å (to 63 Å) in monoolein and 20 Å (to 43 Å) in phytantriol. EAN's unique behaviour is primarily attributed to the amphiphilicity of the cation, which may lower curvature by incorporation into the lipid film as a cosurfactant, as reported previously for surfactant[61] and phospholipid[59,60] systems. EAN and its mixtures with water are also nanostructured liquids with an underlying periodicity of around 10 Å. Larger polar domains may enhance the stability of the phase by better accommodating 4–6 periods of the solvent nanostructure. Further increasing EAN content stabilises the (even less curved but less swollen) lamellar phase, also enabling micelles to form.

The non-amphiphilic EtAN cation is unable to modify film curvature even when present in the polar channels. We predict that longer cation alkyl chains with more pronounced liquid nanostructure, such as propylammonium nitrate, would enhance the observed swelling and also favour micelles sooner.[60,68,69] This effect could also be induced by introducing DES with amphiphilic nanostructure.[70,71]

The lattice parameters of the H_{II} phase of monoolein and both the *Pn*3*m* and H_{II} phases of phytantriol in ChCl : U are also noticeably larger than in water, although the increase in the *Pn*3*m* polar domain diameter of 7 Å (to 30 Å) is less than for EAN. This suggests that the increase may be due to the larger sizes of the solvent components, although some specific interaction of solvent components with lipid head-groups may also alter film curvature. ChCl : U seems to be unique (so far) among neoteric solvents in its ability to support a highly swollen *Pn*3*m* phase *on its own*.

The decrease in ChCl : F and ChCl : CA lattice spacings is similar to the effect of added sugars on the monoolein *Pn*3*m* phase reported by Saturni *et al.*[67] Although they compellingly excluded a *solely* osmotic pressure effect, there may be differences in mixed solvent compositions between the equilibrated lyotropic and excess phases. *i.e.* water may preferentially reside in the region around head-groups – ChCl : U is clearly small enough to fit into the polar channels, but water is preferred once it is present in significant quantities (as the lattice spacing shrinks). The stability of highly curved H_{II} and non-swelling lamellar phases over *Pn*3*m* in ChCl : F and ChCl : CA-rich systems is also consistent with the idea that (non-amphiphilic) nonaqueous solvent components are less effective than water at solvating head groups and swelling bilayer-based lipid phases.

The existence of micelles in EAN, ChCl : F and ChCl : CA initially seems anomalous alongside inverted lyotropic phases. The polarity of neoteric solvents such as these may be determined to be less polar than water by various measures[72,73] (see Table S1, ESI†), leading to a weaker solvophobic effect driving

alkyl chain association. However, as we have noted elsewhere,[16] this also has consequences for forces between surfactant head groups; a lower micelle–solvent interfacial tension favours the larger head-group area that stabilises micelles. Component partitioning around the head groups such as solvation by larger species also increases head-group repulsions and hence area.

It is worth noting that the DES are all treated as a single component, so that DES–water–lipid systems are approximated as pseudo-ternary rather than quaternary systems (Fig. S13 and S14†). This is certainly true for EAN and EtAN, and the strong intermolecular interactions between choline, chloride and urea also make it a reasonable approximation for ChCl : U-containing systems.[74,75] This may not be so in ChCl : F and ChCl : CA, which have larger molecular components whose interactions with ionic species are less specific and/or may be farther from an ideal, deep eutectic composition.

Conclusions

The formation of phytantriol and monoolein liquid crystalline phases in excess solvent is an attractive phenomenon exploited in applications from medical to materials. In water, rapid evaporation of the solvent leads to changes in gel nanostructures, however, in non-volatile, neoteric solvents such as ionic liquids and deep eutectic solvents, there is potential for novel gels for wearable sensors, high temperature syntheses of porous inorganic membranes for energy applications or longer-term stability for soft robotic components. Replacing aqueous solutions with other solvents may lead to new carriers for poorly water-soluble active ingredients, in addition to widening formulation space where these lipids are used in cosmetics or neutraceuticals. We have therefore explored the phase diagrams for two PILs, EAN and EtAN, and three choline chloride-based DES, containing urea, fructose or citric acid. However, within our study, only EAN, EtAN and ChCl : U could be significantly incorporated into the lyotropic cubic phases of either phytantriol or monoolein, probably due to both the size and polarity of the molecular components in these species allowing strong solvation of the lipid headgroups. The amphiphilicity of EAN in particular favours incorporation into the lipid structures, potentially as a co-surfactant. Further studies on a wider range of amphiphilic DES and ionic liquids are needed to develop a fuller understanding of these self-assembled gels which will contribute to their future applications in advanced materials.

Data availability

The data supporting this article have been included as part of the ESI.†

Author contributions

K. J. E. and G. G. W. were involved in the conceptualisation of the experiments and writing the proposal for synchrotron X-ray beamtime access to carry out the SAXS experiment. K. J. E. made samples and conducted the SAXS experiments, carried out the analysis and wrote the original draft for the paper in collaboration with G. G. W. M. T. L. contributed to sample preparation for the SAXS experiment. A. M. D. assisted with data collection during the SAXS experiment. A. M. H. and S. M. set

up the SANS beamline and assisted with SAXS data reduction. K. J. E. and G. G. W. reviewed and edited the manuscript creating the final draft.

Conflicts of interest

The authors declare no conflicts of interest.

Acknowledgements

KJE thanks the University of Sydney for funding a Visiting Professorship. We thank the Australian Synchrotron, part of ANSTO for the provision of beamtime on the SAXS-WAXS beamline (experiment number 13429), and Sophie Goodchild for assisting with the synchrotron data collection. This work was supported by Australian Research Council Discovery Grant DP200102248. We also thank Shurui Miao and Haihui Joy Jiang for making the EAN and EtAN and measuring the water content in some samples.

References

1 C. V. Kulkarni, W. Wachter, G. Iglesias-Salto, S. Engelskirchen and S. Ahualli, *Phys. Chem. Chem. Phys.*, 2011, **13**, 3004–3021.
2 J. Barauskas and T. Landh, *Langmuir*, 2003, **19**, 9562–9565.
3 N. Bennett, A. M. Seddon, J. E. Hallett, W. Kockelmann, V. P. Ting, S. Sadasivan, R. P. Tooze and S. R. Hall, *APL Mater.*, 2016, **4**, 015701.
4 S. D. Kaur, G. Singh, G. Singh, K. Singhal, S. Kant and N. Bedi, *Journal of Pharmaceutical Research International*, 2021, **33**, 118–135.
5 T. M. Hinton, F. Grusche, D. Acharya, R. Shukla, V. Bansal, L. J. Waddington, P. Monaghan and B. W. Muir, *Toxicol. Res.*, 2014, **3**, 11–22.
6 T. Kanti Maiti, W. Liu, A. Niyazi, A. M. Squires, S. Chattpoadhyay and M. Di Lorenzo, *Biosensors*, 2024, **14**, 289.
7 S. Akbar, J. M. Elliott, M. Rittman and A. M. Squires, *Adv. Mater.*, 2013, **25**, 1160–1164.
8 X. Lai, Y. Ding, C.-M. Wu, X. Chen, J.-h. Jiang, H.-Y. Hsu, Y. Wang, A. P. Le Brun, J. Song, M.-L. Han, J. Li and H.-H. Shen, *ACS Appl. Mater. Interfaces*, 2020, **12**, 44485–44498.
9 S. P. Akhlaghi, L. B. da Silveira Balestrin, C. Brinatti, F. Pirolt, W. Loh and O. Glatter, *J. Pharm. Sci.*, 2020, **109**, 2024–2032.
10 M. Kitaoka, A. Oka and M. Goto, *Pharmaceutics*, 2020, **12**, 814.
11 M. Basu, P. A. Hassan and S. B. Shelar, *J. Mol. Liq.*, 2023, **375**, 121301.
12 N. V. P. Veríssimo, C. U. Mussagy, H. B. S. Bento, J. F. B. Pereira and V. d. C. Santos-Ebinuma, *Biotechnol. Adv.*, 2024, **71**, 108316.
13 J.-P. Belieres and C. A. Angell, *J. Phys. Chem. B*, 2007, **111**, 4926–4937.
14 D. F. Evans, A. Yamauchi, R. Roman and E. Z. Casassa, *J. Colloid Interface Sci.*, 1982, **88**, 89–96.
15 D. F. Evans, A. Yamauchi, G. J. Wei and V. A. Bloomfield, *J. Phys. Chem.*, 1983, **87**, 3537–3541.
16 J. B. Marlow, R. Atkin and G. G. Warr, *J. Phys. Chem. B*, 2023, **127**, 1490–1498.
17 T. L. Greaves, D. F. Kennedy, S. T. Mudie and C. J. Drummond, *J. Phys. Chem. B*, 2010, **114**, 10022–10031.

18 A. Dolan, R. Atkin and G. G. Warr, *Chem. Sci.*, 2015, **6**, 6189–6198.
19 S. J. Bryant, K. Wood, R. Atkin and G. G. Warr, *Soft Matter*, 2017, **13**, 1364–1370.
20 M. T. Lam, W. D. Adamson, S. Miao, R. Atkin and G. G. Warr, *J. Colloid Interface Sci.*, 2019, **552**, 597–603.
21 R. Hayes, S. Imberti, G. G. Warr and R. Atkin, *Phys. Chem. Chem. Phys.*, 2011, **13**, 3237–3247.
22 R. Hayes, S. Imberti, G. G. Warr and R. Atkin, *J. Phys. Chem. C*, 2014, **118**, 13998–14008.
23 D. O. Abranches and J. A. P. Coutinho, *Annu. Rev. Chem. Biomol. Eng.*, 2023, **14**, 141–163.
24 Q. Zhang, K. De Oliveira Vigier, S. Royer and F. Jerome, *Chem. Soc. Rev.*, 2012, **41**, 7108–7146.
25 D. V. Wagle, H. Zhao and G. A. Baker, *Acc. Chem. Res.*, 2014, **47**, 2299.
26 O. Długosz, *Materials*, 2023, **16**, 627.
27 M. Wysokowski, R. K. Luu, S. Arevalo, E. Khare, W. Stachowiak, M. Niemczak, T. Jesionowski and M. J. Buehler, *Chem. Mater.*, 2023, **35**, 7878–7903.
28 A. Sharma, Y. R. Park, A. Garg and B.-S. Lee, *J. Med. Chem.*, 2024, **67**, 14807–14819.
29 J. S. Almeida, E. V. Capela, A. M. Loureiro, A. P. M. Tavares and M. G. Freire, *ChemEngineering*, 2022, **6**, 51.
30 Y. H. Choi, J. van Spronsen, Y. Dai, M. Verberne, F. Hollmann, I. W. C. E. Arends, G.-J. Witkamp and R. Verpoorte, *Plant Physiol.*, 2011, **156**, 1701–1705.
31 G. G. Warr and R. Atkin, *Curr. Opin. Colloid Interface Sci.*, 2020, **45**, 83–96.
32 Q. Li, J. Wang, N. Lei, M. Yan, X. Chen and X. Yue, *Phys. Chem. Chem. Phys.*, 2018, **20**, 12175–12181.
33 O. S. Hammond, N. S. Elstone, J. Doutch, P. Li and K. J. Edler, *Nanoscale*, 2023, **15**, 19314–19321.
34 R. S. Atri, A. Sanchez-Fernandez, O. S. Hammond, I. Manasi, J. Doutch, J. P. Tellam and K. J. Edler, *J. Phys. Chem. B*, 2020, **124**, 6004–6014.
35 T. Arnold, A. J. Jackson, A. Sanchez-Fernandez, D. Magnone, A. E. Terry and K. J. Edler, *Langmuir*, 2015, **31**, 12894–12902.
36 A. Sanchez-Fernandez, A. J. Jackson, S. F. Prévost, J. J. Doutch and K. J. Edler, *J. Am. Chem. Soc.*, 2021, **143**, 14158–14168.
37 A. Sanchez-Fernandez, O. S. Hammond, K. J. Edler, T. Arnold, J. Doutch, R. M. Dalgliesh, P. Li, K. Ma and A. J. Jackson, *Phys. Chem. Chem. Phys.*, 2018, **20**, 13952–13961.
38 S. J. Bryant, R. Atkin and G. G. Warr, *Soft Matter*, 2016, **12**, 1645–1648.
39 S. J. Bryant, R. Atkin and G. G. Warr, *Langmuir*, 2017, **33**, 6878–6884.
40 S. N. Pedro, M. S. M. Mendes, B. M. Neves, I. F. Almeida, P. Costa, I. Correia-Sá, C. Vilela, M. G. Freire, A. J. D. Silvestre and C. S. R. Freire, *Pharmaceutics*, 2022, **14**, 827.
41 Y. Chen, G. Hong, L. Li, Q. Qu, G. Li, J. Wu and L. Ge, *Chem. Eng. J.*, 2024, **483**, 149344.
42 S. J. Bryant, M. A. da Silva, K. M. Z. Hossain, V. Calabrese, J. L. Scott and K. J. Edler, *Nanoscale Adv.*, 2021, **3**, 2252–2260.
43 S. J. Bryant, E. K. Bathke and K. J. Edler, *J. Colloid Interface Sci.*, 2021, **601**, 98–105.

44 S. J. Bryant, A. Elbourne, T. L. Greaves and G. Bryant, *J. Mater. Chem. B*, 2023, **11**, 6868–6880.
45 T. L. Greaves, A. Weerawardena, C. Fong and C. J. Drummond, *J. Phys. Chem. B*, 2007, **111**, 4082–4088.
46 T. L. Greaves, A. Weerawardena, C. Fong, I. Krodkiewska and C. J. Drummond, *J. Phys. Chem. B*, 2006, **110**, 22479–22487.
47 X. Mulet, D. F. Kennedy, T. L. Greaves, L. J. Waddington, A. Hawley, N. Kirby and C. J. Drummond, *J. Phys. Chem. Lett.*, 2010, **1**, 2651–2654.
48 S. Fujiwara, H. Ohno and T. Ichikawa, *Mol. Syst. Des. Eng.*, 2018, **3**, 668–676.
49 J. Zhai, S. Sarkar, N. Tran, S. Pandiancherri, T. L. Greaves and C. J. Drummond, *J. Phys. Chem. Lett.*, 2021, **12**, 399–404.
50 S. T. Mudie, *scatterBrain v1.15*, **https://archive.synchrotron.org.au/aussyncbeamlines/saxswaxs/software-saxswaxs**.
51 X. Meng, K. Ballerat-Busserolles, P. Husson and J.-M. Andanson, *New J. Chem.*, 2016, **40**, 4492–4499.
52 A. P. Abbott, G. Capper, D. L. Davies, R. K. Rasheed and V. Tambyrajah, *Chem. Commun.*, 2003, 70–71.
53 L. P. Silva, L. Fernandez, J. H. F. Conceição, M. A. R. Martins, A. Sosa, J. Ortega, S. P. Pinho and J. A. P. Coutinho, *ACS Sustainable Chem. Eng.*, 2018, **6**, 10724–10734.
54 E. A. Crespo, L. P. Silva, M. A. R. Martins, M. Bülow, O. Ferreira, G. Sadowski, C. Held, S. P. Pinho and J. A. P. Coutinho, *Ind. Eng. Chem. Res.*, 2018, **57**, 11195–11209.
55 M. H. Shafie, R. Yusof and C.-Y. Gan, *J. Mol. Liq.*, 2019, **288**, 111081.
56 H. Qiu and M. Caffrey, *Biomaterials*, 2000, **21**, 223–234.
57 B. Hammouda, *Probing Nanoscale Structures – the SANS Toolbox*, Gaithersburg, MD, 2010, **https://www.ncnr.nist.gov/staff/hammouda/the_sans_toolbox.pdf**.
58 Y.-D. Dong, A. W. Dong, I. Larson, M. Rappolt, H. Amenitsch, T. Hanley and B. J. Boyd, *Langmuir*, 2008, **24**, 6998–7003.
59 L. Salvati Manni, C. Davies, K. Wood, S. Assenza, R. Atkin and G. G. Warr, *J. Colloid Interface Sci.*, 2023, **643**, 276–281.
60 L. Salvati Manni, W.-K. Fong, K. Wood, N. Kirby, S. Seibt, R. Atkin and G. G. Warr, *J. Colloid Interface Sci.*, 2024, **657**, 320–326.
61 S. J. Bryant, C. J. Jafta, R. Atkin, M. Gradzielski and G. G. Warr, *J. Colloid Interface Sci.*, 2019, **540**, 515–523.
62 D. C. Turner, Z.-G. Wang, S. M. Gruner, D. A. Mannock and R. N. McEllianey, *J. Phys. II*, 1992, **2**, 2039–2063.
63 J. Briggs, H. Chung and M. Caffrey, *J. Phys. II*, 1996, **6**, 723–751.
64 R. Hayes, S. Imberti, G. G. Warr and R. Atkin, *Angew. Chem., Int. Ed.*, 2012, **51**, 7468–7471.
65 T. L. Greaves, D. F. Kennedy, A. Weerawardena, N. M. K. Tse, N. Kirby and C. J. Drummond, *J. Phys. Chem. B*, 2011, **115**, 2055–2066.
66 K. Larsson, K. Fontell and N. Krog, *Chem. Phys. Lipids*, 1980, **27**, 321–328.
67 L. Saturni, F. Rustichelli, G. M. Di Gregorio, L. Cordone and P. Mariani, *Phys. Rev. E:Stat., Nonlinear, Soft Matter Phys.*, 2001, **64**, 040902.
68 R. Hayes, S. Imberti, G. G. Warr and R. Atkin, *Phys. Chem. Chem. Phys.*, 2011, **13**, 13544–13551.
69 T. Murphy, R. Hayes, S. Imberti, G. G. Warr and R. Atkin, *Phys. Chem. Chem. Phys.*, 2016, **18**, 12797–12809.

70 S. McDonald, T. Murphy, S. Imberti, G. G. Warr and R. Atkin, *J. Phys. Chem. Lett.*, 2018, **9**, 3922–3927.
71 I. Manasi, R. Schweins, K. Ma and K. J. Edler, *Langmuir*, 2023, **39**, 16776–16784.
72 T. L. Greaves, A. Weerawardena and C. J. Drummond, *Phys. Chem. Chem. Phys.*, 2011, **13**, 9180–9186.
73 I. L. Topolnicki, P. A. FitzGerald, R. Atkin and G. G. Warr, *ChemPhysChem*, 2014, **15**, 2485–2489.
74 O. S. Hammond, D. T. Bowron and K. J. Edler, *Angew. Chem., Int. Ed.*, 2017, **56**, 9782–9785.
75 M. M. Nolasco, S. N. Pedro, C. Vilela, P. D. Vaz, P. Ribeiro-Claro, S. Rudić, S. F. Parker, C. S. R. Freire, M. G. Freire and A. J. D. Silvestre, *Frontiers in Physics*, 2022, **10**, 834571.

